Membrane and Water Treatment, *Vol. 15, No. 4 (2024) 163-176*
https://doi.org/10.12989/mwt.2024.15.4.163

Preparation and characterization of PVDF Flat sheet membrane for VMD: Effect of different non-solvent additives and solvents in dope solution

Meenakshi Yadav*, Sushant Upadhyaya and Kailash Singh**

Department of Chemical Engineering, Malaviya National Institute of Technology Jaipur-302017, India

(Received July 3, 2024, Revised September 4, 2024, Accepted September 5, 2024)

Abstract. Asymmetric flat sheet poly(vinylidene fluoride) (PVDF) membranes were fabricated using the phase inversion technique, employing four distinct solvents with varying solubility power: N, N-dimethylacetamide (DMAc), N, N-dimethylformamide (DMF), Dimethyl sulfoxide (DMSO), and N-Methyl-2-pyrrolidone (NMP). The influence of these solvents on the crystalline properties of the polymers was investigated using X-ray diffraction (XRD) and Fourier-transform infrared spectroscopy (FT-IR) to elucidate their role in PVDF polymorphism during membrane formation. Our findings revealed significant variations in membrane crystalline phase due to the dissolution of PVDF in different solvents, with α-polymerization predominant in membranes cast with NMP and DMSO, while DMF and DMAc solvents favored β-type polymerization. Further, various additives including PEG-400, TiO2, LiCl, LiBr, acetone, ethanol, propanol, and water were employed to evaluate their impact on membrane morphology and properties. Scanning electron microscopy (SEM) and Ultimate testing machine (UTM) were utilized to analyze membrane morphology, while the tensile strength, contact angle, pore size, and porosity were estimated using the sessile drop method, imageJ, and gravimetric method, respectively. Our results demonstrated that all additives exerted influence on membrane morphology and properties depending on their characteristics and interactions with solvents and polymers. Notably, acetone, being volatile, facilitated the formation of a thin PVDF layer on the membrane surface, resulting in a reduced average pore size (0.18μm). Conversely, LiCl and LiBr acted as pore-forming additives, yielding membranes with distinct pore characteristics and porosity. Moreover, water as a non-solvent additive induced pregelation during the nonsolvent-induced phase separation (NIPS) process, thereby promoting pore formation (53% porosity) and enhancing membrane hydrophobicity (104° contact angle). To evaluate the quality of synthesized membranes, permeate flux ranging from 16.2 L/m^2.hr to 27.9 L/m^2.hr with a salt rejection rate of 98 %, was evaluated using Vacuum Membrane Distillation (VMD).

Keywords: additives; desalination; hydrophobicity; NIPS; PVDF; solvent; vacuum membrane distillation

1. Introduction

Membrane distillation (MD) stands out as a highly promising next-generation technology for desalination and wastewater treatment due to its robust capabilities and distinctive mechanism. Unlike conventional processes, MD operates as a non-isothermal membrane process, leveraging the vapor pressure difference across a porous hydrophobic membrane driven by temperature gradients between feed and permeation solutions (Kalla 2020). Among the four distinct MD configurations - direct contact membrane distillation (DCMD), vacuum membrane distillation (VMD), sweeping gas membrane distillation (SGMD), and air gap membrane distillation (AGMD) - VMD emerges as a popular and cost-effective option in membrane separation technology (Baghel *et al*. 2017, Gryta 2011, Zoungrana *et al*. 2016, Loussif and Orfi 2016). This technology capitalizes on liquid-vapor phase equilibrium principles, maintaining a vapor pressure difference by applying a vacuum to the permeate side, thereby enhancing flux through the membrane. VMD not only facilitates process selectivity, enabling the removal of volatile components, but has also found utility in desalination applications (Hou *et al*. 2023, Kalla 2020).

Polymeric membranes have garnered considerable attention in MD technology for their ease of manufacture, tunable properties, and cost-effectiveness (Tibi *et al*. 2020). Hydrophobic materials such as polypropylene (PP), poly-tetrafluoroethylene (PTFE), and polyvinylidene fluoride (PVDF) constitute the predominant membrane materials, with PVDF emerging as a primary choice owing to its superior mechanical strength, excellent chemical resistance, and high hydrophobicity (Li *et al*. 2019, X. Wang *et al*. 2023). Moreover, PVDF's compatibility with various organic solvents renders it versatile for membrane fabrication via diverse phase conversion processes, including evaporation-induced phase separation (EIPS), thermally induced phase separation (TIPS), vapor-induced phase separation (VIPS), and non-solvent-induced phase separation (NIPS) (Jung *et al*. 2016, Tofighy *et al*. 2021). Among these, the NIPS method is particularly favored for its versatility and cost-effectiveness (Junoh *et al*. 2021).

In recent years, significant attention has been directed towards enhancing PVDF membrane performance through optimization and refinement. Researchers have primarily focused on membrane fabrication conditions, including

*Corresponding author, Ph.D.,
E-mail: 2018rch9037@mnit.ac.in

**Co-corresponding author, Professor

ISSN: 2005-8624 (Print), 2092-7037 (Online)

membrane dope solutions (e.g., polymer concentration, additives, solvent type, solution viscosity) and casting conditions (e.g., casting temperature, coagulation bath composition and temperature, drying methods), as these factors profoundly influence PVDF membrane characteristics (Feng *et al*. 2006, Liu *et al*. 2021). Notably, the composition of the casting solution, especially the choice of solvent, emerges as a critical factor due to its potential to alter polymer solvation power and impact kinetic and thermodynamic properties of the casting solution (Kang *et al*. 1991, Rasool and Vankelecom 2021, Pan *et al*. 2020). Various solvents, including N-methyl-2-pyrrolidone (NMP), dimethyl sulfoxide (DMSO), dimethylacetamide (DMAc), dimethylformamide (DMF), have been employed for PVDF membrane fabrication, each possessing distinct chemical and physical properties that can influence interactions with polymer and additives, thereby affecting phase inversion processes and resulting in membranes with diverse characteristics.

In addition to solvents, non-solvent additives wield significant potential to affect the kinetic and thermodynamic interplay between solvent and non-solvent, thereby influencing membrane morphology. These additives encompass macromolecular polymeric additives, macromolecular salts, alcohols, organic and inorganic acids, and strong non-solvent additives like water. Macromolecular additives, such as polyethylene glycol (PEG), Polyvinyl pyrrolidone (PVP), and cellulose acetate (CA), are commonly employed as pore-forming additives in PVDF membranes (Kamarudin *et al*. 2021, J. Wang *et al*. 2016, Rasool and Vankelecom 2021). However, the choice of additives warrants careful consideration, as incomplete leaching during the coagulation and washing process may affect membrane properties. Therefore, water-soluble organic and inorganic macromolecular additives have emerged as preferred options for membrane preparation due to their compatibility with the hydrophobic nature of PVDF.

This study aims to explore the effects of different solvents, including NMP, DMAc, DMF, and DMSO, as well as non-solvent additives, on the performance of microporous hydrophobic flat sheet PVDF membranes. The investigation involves comprehensive characterization using scanning electron microscopy (SEM), Fourier-transform infrared spectroscopy (FTIR), X-ray diffraction (XRD), and contact angle measurement techniques. Furthermore, the study evaluates the influence of additives and solvent types on membrane morphology and properties, including porosity, hydrophobicity, and mechanical strength.

2. Thermodynamic and kinetic theory of the membrane

Throughout this experimental analysis, we are interested in recycling used membranes for utilization in wastewater.

2.1 Thermodynamic equilibrium (Liquid-liquid phase separation and gelation)

The phase diagram depicting the relationship among polymer, solvent, and non-solvent serves as a valuable tool for investigating the thermodynamic aspects of membrane formation processes. Thermodynamic equilibrium can be quantified by parameters such as the Gibbs free energy change (ΔG) during phase separation. For instance, a higher ΔG value indicates a more stable dope solution, requiring a greater amount of non-solvent to reach the binodal line and induce phase separation. Thermodynamic equilibrium fundamentally governs the stability of the dope solution, a stable solution is characterized by an increased gap between the binodal line and the solvent-polymer phase line, indicative of an expanded stable region within the phase diagram (see Fig.1) (Yadav *et al*. 2022). In such instances, a considerable amount of non-solvent is necessary to induce precipitation, leading to the development of a dense morphology in the resulting membrane.

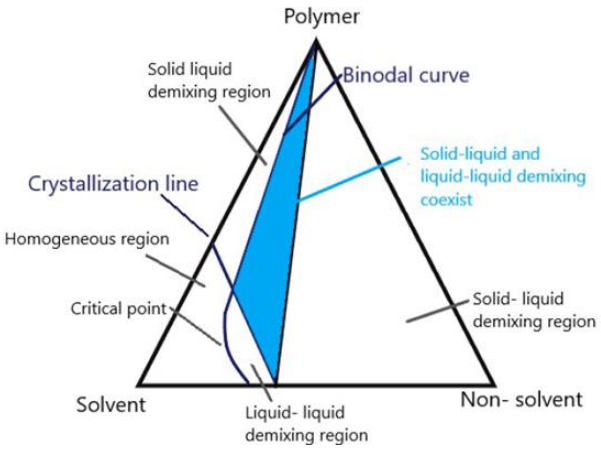

Fig. 1 Phase diagram of solvent and non-solvent for NIPS

Conversely, a diminished gap between the binodal line and the solvent-polymer phase line signifies an increase in the unstable region. This scenario necessitates less non-solvent to trigger liquid-liquid phase separation. The phase boundary delineates the threshold of nonsolvent content that the polymer system can withstand without undergoing precipitation, thus dictating the theoretical porosity based on thermodynamic principles. Additionally, the cloud point curve, obtained by plotting the temperature against the polymer concentration at which phase separation occurs, provides quantitative insight into the thermal stability of the dope solution.The gelation time required for membrane solidification during the wet phase significantly impacts polymer precipitation rates, thereby influencing membrane structure. The thermodynamics of phase inversion are quantified through the cloud point of the polymer dope solution. Variation in solvent type and the incorporation of non-solvent additives into the polymer dope solution induce shifts in the binodal line within the phase diagram, thereby exerting pronounced effects on membrane morphology.

2.2 Kinetic effect (The rate of exchange of solvent and non-solvent)

The kinetics of solvent and non-solvent exchange during coagulation in the Non-Solvent Induced Phase Separation (NIPS) process play a critical role in elucidating and

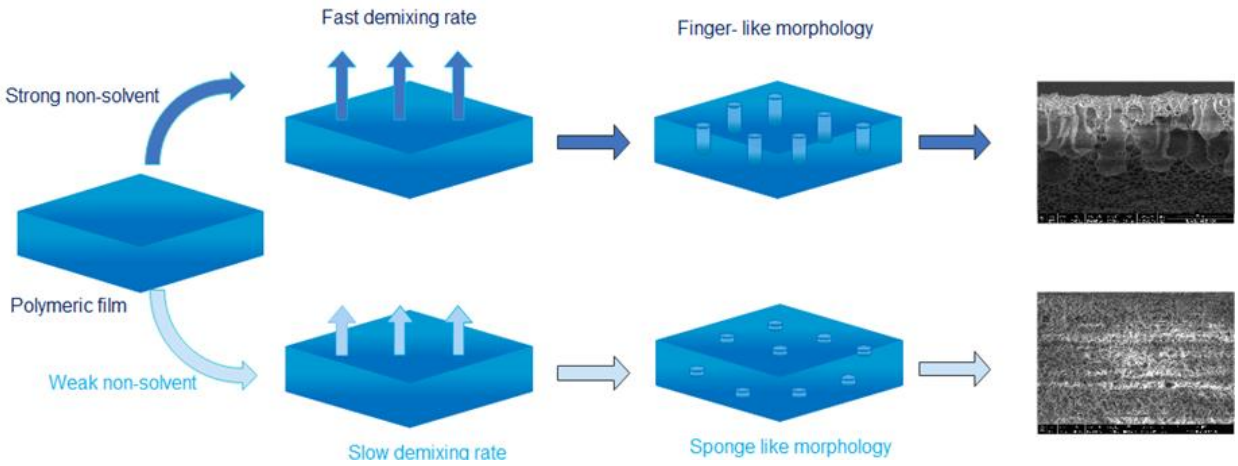

Fig. 2 Kinetic effect of non-solvent on membrane morphology of membrane

regulating membrane structure. Quantitative analysis of solvent exchange kinetics can be conducted using Fick's law of diffusion, where the diffusion coefficient (D) is determined by measuring the concentration gradient of solvent across the membrane interface. Monitoring the composition of the coagulation bath allows for a comprehensive study of phase separation kinetics. Upon immersion of the casted membrane into the coagulation bath during the membrane preparation process, the polymeric solution swiftly segregates into two distinct phases: a polymer-rich phase and a polymer-poor phase. The polymer-rich phase forms the thin top layer of a symmetric membrane, with pores primarily formed via nucleation and growth mechanisms within the dilute polymer phase.The nature of the solvent and its interaction with the non-solvent profoundly influence the exchange rate kinetics. The rate of phase separation can be quantitatively described by the diffusion rate, which is influenced by factors such as solvent viscosity and temperature. A rapid exchange rate tends to yield deep, finger-like pores, whereas a slower rate results in the formation of smaller, sponge-like pores (Yadav *et al*. 2024). Further reduction in the exchange rate leads to the formation of a dense membrane, as depicted in Fig.2. Additionally, the properties of additives, particularly their solubility in the non-solvent, impact pore size and membrane porosity.

3. Material and methods

3.1 Materials

Polyvinyl difluoride (PVDF) powder (specific gravity-1.77-1.79) was obtained from Sita chemicals Pvt., Ltd. (India). N-methyl-2-pyrrolidone (NMP), dimethyl sulfoxide (DMSO), dimethylacetamide (DMAc) (density of 0.940 g/ml), dimethylformamide (DMF) were purchased from TECH INC India Pvt. Ltd and has been used as a solvent to dissolve PVDF powder to prepare the dope solution. Ethanedi-ol, propanol, acetone, TiO_2, $AlCl_3$, LiCl, LiBr, PEG- 400, and H_2O as an additive were purchased from Savita Chemical Co., Ltd. (India). The non-woven fabric used as membrane support (0.1mm thick) was purchased from Permionics Membranes Pvt.Ltd, Vadodara, to avoid shrinkage of the membrane during phase inversion. Double distilled water was used throughout the experimental procedures as the coagulant bath.

3.2 Dope solution preparation

A different set of dope solutions was prepared to consist of parent polymer, PVDF powder (16 wt%) in four different solvents: DMAc, DMSO, NMP, and DMF. These solutions are labeled as MS-1, MS-2, MS-3, and MS-4, corresponding to the solvents NMP, DMSO, DMAc, and DMF, respectively, without any additives. Additionally, ten different dope solutions using DMAc as the solvent and 16 wt % PVDF along with different additives (PEG-400, TiO2, LiCl, LiBr, AlCl3, acetone, ethanol, propanol, and H2O) were prepared for studying the effect of different additives during the formation of porous structure flat sheet PVDF membrane. These solutions, labeled from M0-1 to MA-9 in Table 1, include one dope solution without additives (M0-1) and nine with various additives (MA-1 to MA-9).

The PVDF powder is dried in an oven for 12 hours at 60 °C to remove the moisture prior to further synthesis. The dried PVDF is then been added to the solvent, to achieve 16 wt % PVDF in 100 gm dope solution. Then, the solution was placed on temperature controlled magnetic stirrer and vigorously stirred for 24 hours at 70°C until a homogenous dope solution was produced. Subsequently, the solution was left for 6 hours without agitation for degassing at room temperature, to remove bubbles in the dope solution. This process was followed for all fourteen solutions, ensuring consistent preparation conditions. Table 1 summarizes the composition of the prepared dope solution with different additives and solvents.

3.3 Porous PVDF membrane fabrication

Porous PVDF flat sheet membranes were prepared via phase inversion techniques by a single casting step. Firstly, the non-woven fabric was fixed on the glass plate to provide a smooth surface for membrane casting and the glass plate was fixed over the membrane casting machine. About 20 ml of prepared dope solution was poured homogenously into

Table 1 Membrane code and Compositions of the polymer solutions for membrane casting. (PVDF concentration= 16 wt%)

S.no	Membrane code	Additive	Solvent
1.	MS-1	-	NMP (84 wt%)
2.	MS-2	-	DMSO (84 wt%)
3.	MS-3	-	DMAc (84 wt%)
4.	MS-4	-	DMF (84 wt%)
5.	M0-1	-	DMAc (84 wt%)
6.	MA-1	PEG-400 (4 wt%)	DMAc (80 wt%)
7.	MA-2	TiO_2 (4 wt%)	DMAc (80 wt%)
8.	MA-3	LiCl (4 wt%)	DMAc (80 wt%)
9.	MA-4	LiBr (4 wt%)	DMAc (80 wt%)
10.	MA-5	$AlCl_3$ (4 wt%)	DMAc (80 wt%)
11.	MA-6	Acetone (4 wt%)	DMAc (80 wt%)
12.	MA-7	Ethanol (4 wt%)	DMAc (80 wt%)
13.	MA-8	Propanol (4 wt%)	DMAc (80 wt%)
14.	MA-9	H_20 (4 wt%)	DMAc (80 wt%)

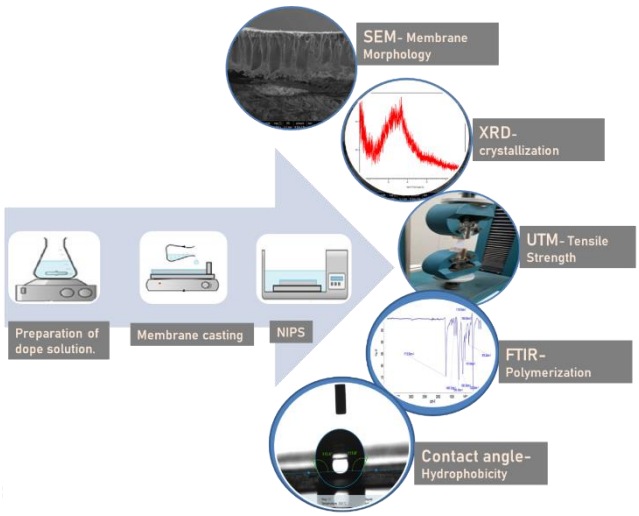

Fig. 3 Membrane preparation and characterization technique

the trapezoidal channel of the sheet casting machine and the membrane was cast over the non-woven fabric with the help of a pulling blade attached to the trapezoidal channel in the machine. The gap between the blade and non-woven fabric was kept at 200 microns to maintain the thickness of the membrane. At room temperature, the casted polymeric thin film along with the glass plate was fully submerged in the coagulant bath containing 500 ml distilled water. During the phase inversion process, the polymeric thin film gets separated into the polymer-rich phase and polymer-poor phase, which is responsible for its porous structure. The membrane was kept dipped in the coagulation bath for 24 hours to ensure the complete removal of the remaining solvent. Finally, the synthesized flat sheet membranes were dried in a dryer overnight before further treatment. The designations for each membrane were tabulated in Table 1, accordingly. Membrane preparation and its characterization techniques are shown in Fig. 3.

3.4 Viscosity of dope solution

The viscosity of the casting dope solution was measured using a rotating viscometer (Labman- (LMDV- 60)) using Spindal L-4 at a rotation speed of 1.5 rpm. The degassed dope solution was first poured into the cylindrical vessel and then the spindle was submerged in the solution. One by one, the casting dope solutions were poured into a cylindrical vessel which was then loaded into the chamber of the viscometer. Once the spindle began rotating, the viscosity of the dope solution upon stabilization was measured after 2 minutes to stabilize the values. All the measurements were made at room temperature.

3.5 Morphology and pore size

Scanning electron microscopy (SEM, Hitachi SU8020) of magnification range ×100 to ×1,0, 000 was used to study the morphology of the prepared PVDF membrane samples under high magnification to understand the overall micro-structure of the membranes. All the samples were cut into a square coupon and then frozen in liquid nitrogen to break them up cross-sectionally, to study the cross-sectional microstructure of the membranes. Moreover, membrane samples were sputter coated with gold to form a conductive layer of gold over the sample surface before being tested as the polymeric film is non-conductive. Their SEM images at cross-section and surface were captured at various magnifications to find the correlation between morphological structure overuse of different additives and different solvents in PVDF membrane.

These SEM images were further analyzed using image processing software- Jimage software to find the pore size distribution, maximum pore size, and average pore size. The equivalent diameter of membrane pores was calculated based on the area (A) estimated by the image processing software. The area A represents the cross-sectional area of each pore as detected in the SEM images. Assuming the pores to be circular, the equivalent diameter (d_{eq}) is calculated using the formula Eq. (1) (Phattaranawik *et al.* 2003):

$$d_{eq} = \sqrt{A/\pi} \quad (1)$$

In this equation, AAA is the area of the pore, and π\piπ is the mathematical constant representing the ratio of a circle's circumference to its diameter. By assuming circular pores, this formula provides a simple and effective way to estimate the diameter of pores from their area as seen in SEM images.

3.6 Porosity

The total porosity of the membrane can be defined as the total volume of membrane pores divided by membrane volume, it was calculated by using a gravimetric method. In this method, each casted membrane was cut into square coupons of dimension 2×2 cm^2 followed by weighting the membrane before and after immersing it into an isopropanol solution for 24 hours at room temperature so that the

solvent could penetrate completely inside the pores of the membrane. This method measures total porosity as it accounts for both interconnected and isolated pores within the membrane structure. Eq. (2), has been employed for the calculation of PVDF membrane porosity (Yadav *et al*. 2023).

$$\varepsilon = \frac{(\omega_1 - \omega_2)/D_i}{(\omega_1 - \omega_2)/D_i + \omega_2/D_p} \quad (2)$$

where, ω_1, ω_2, D_i and D_p are the weight of the wet membrane in g, the weight of the dry membrane in g, iso-propanol density in g/m^3, and polymeric membrane density in g/m^3, respectively.

3.7 Hydrophobicity

Hydrophobicity measurement of the prepared membrane was adhered to investigate the surface of these membranes using static contact angle (θ) measurement procedures. The membrane square coupons of size 1 cm × 1 cm were prepared and then tested using Drop Shape Analyzer (DSA25) Mk2 of firm Kruss, Germany. The prepared membrane samples were clamped to the sample holder and a deionized water droplet of volume 4µl was placed over the flat surface of the membrane. With the help of Kruss' advanced drop shape analyzer, the geometrical angle between the hydrophobic surface and water droplet was measured after 30 seconds and the average data was taken for at least 5 different membrane samples.

3.8 Mechanical strength

The mechanical properties of PVDF membrane samples like tensile strength and elongation at the break of the membrane were measured using Universal Testing Machine (UTM) with a starting gauge length of 50 mm of membrane strip of dimension 8 cm × 2 cm, and a stretching rate of 10 mm/min. The average values were obtained from five tests conducted for each sample.

4. Result and discussion

The fabricated membrane morphology, crystalline phase, wetting characteristics, porosity, and mechanical properties are investigated thoroughly by implementing phase inversion process. Primarily, the effect of solvent and additive in dope solution on membrane characteristics is understood by using various analytical techniques such as AFM, SEM, FTIR, sessile drop method, gravimetric method, and UTM. The scientific findings are discussed in detail in the subsequent sections.

4.1 Effect of solvent:

The selection of solvent is considered as an important parameter for synthesizing a flat sheet hydrophobic membrane suitable for VMD. Solvent plays an important role in determining the thermodynamic and kinetic parameters, including the interaction between the polymer and solvent, as well as the interaction between the solvent and nonsolvent in NIPS process of membrane synthesis (García-Fernández *et al*. 2014, Mohsenpour *et al*. 2016, Sadrzadeh and Bhattacharjee 2013).

4.1.1 Effect on solubility parameter, polymorphism and membrane morphology

In this study four different solvents namely, N-methyl-2-pyrrolidone (NMP), dimethyl sulfoxide (DMSo), dimethylacetamide (DMAc), and dimethylformamide (DMF) were selected for identifying the effect of solvent on characteristics of synthesized MD membrane. The comparative study was performed for each solvent on the basis of solubility parameter, polymorphism, porosity (ϵ), Contact angle (θ), Tensile strength (TS), Liquid entry pressure (LEP) and pore size (d_p).

Relative solubility of solvent with PVDF and water is evaluated by Hansen's solubility parameter HSP distance, (R_{HSP}), which includes a polar component δ_d, a dispersion force component δ_p, and a hydrogen bonding component δ_h (García-Fernández *et al*., 2014). The interaction between PVDF and the solvent can be given as HSP distance (R_{HSP}) by equation 3 (Hansen 1967).

$$R_{HSP} = \sqrt{4(\delta d_1 - \delta d_2)^2 + (\delta p_1 - \delta p_2)^2 + (\delta h_1 - \delta h_2)^2} \quad (3)$$

where, subscripts *1* and *2* refer to the solvent and the polymer PVDF, respectively. The lower the distance R_{HSP}, shows better solubility between solvent and polymer. The solubility parameter of four different solvents DMAc, NMP, DMSO, and DMF with PVDF polymer is listed in Table 2. It was observed that the value of R_{HSP} the solvent–polymer pair of DMAc and PVDF is smaller than those of other solvents, indicating that the affinity of PVDF with DMAc is better than other solvents. According to the equilibrium thermodynamic, for a strong solvent having a lower value R_{HSP}, results in a increases in the stability of the polymeric dope solution (Arefi-Oskoui *et al*. 2017). Therefore, DMAc is considered to be the best solvent to dissolve PVDF to make a stable dope solution.

For further investigation in order to determine the bonding crystalline structure of synthesized PVDF membrane made from different solvents, the XRD and FTIR analysis was performed. The FTIR analysis provides valuable information about the structure of PVDF membrane allowing it to distinguish between the different crystalline forms. As shown in Fig. 4.1, M-DMAc shows peaks on 486 and 760, which are characteristic peaks for α-type polymerization, whereas a peak on 840 shows the presence of β-type polymerization. The membrane prepared with NMP as solvent shows only α-type polymerization with peaks at 760 and 486 wavelengths. DMF membrane is showing peaks on 486 and 760 wavelengths, showing the presence of both α polymerizations along with a peak at 840, which confirms the presence of β polymerization.

From the Fig. 4(b) it is clear that, NMP is showing strong diffraction peaks at 20.09 and 26.15, which correspond to (1 1 0) and (0 2 1) planes of PVDF crystals in the α phase, respectively. This result reveals that the non-

Table 7 Diffusion of flow rates of treated membranes

Solvent	δ_d	δ_p	δ_h	R_{HSP} (P-S)	R_{HSP} (W-S)
Water	15.5	16	42.3		
NMP	18	12.3	7.2	2.5690	35.64
DMSo	18.4	16.4	10.2	4.6872	32.62
DMAc	16.8	11.5	10.2	1.6248	32.51
DMF	17.4	13.7	11.3	2.4515	31.31
PVDF	17.2	12.5	9.2		

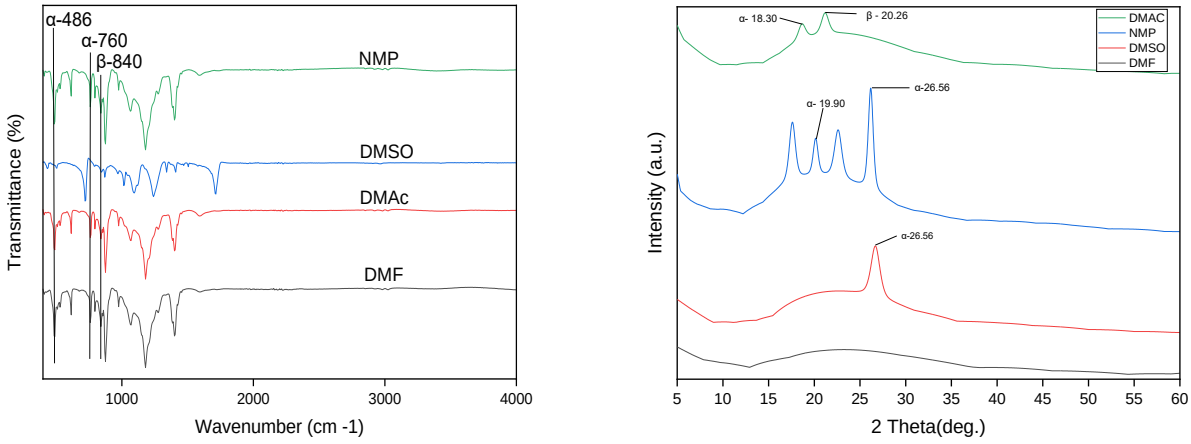

(a) FTIR (b) XRD

Fig. 4 FTIR and XRD pattern of membrane prepared with different solvents showing the polymerization

Table 5 Polymerization structure of PVDF and their XRD and FTIR peaks

S.no	Polymerization	Structure	XRD peaks		FTIR wavenumber (cm^{-1})
			2θ	Crystal plane	
1.	α	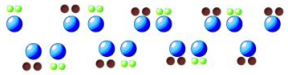	17.66◦ 18.30◦ 19.90◦ 26.56◦	(1 0 0) (0 2 0) (1 1 0) (0 2 1)	408,532,614,766, 795,855, 976
2.	β	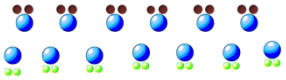	20.26◦	(1 1 0) (2 0 0)	510,840,1279
3.	γ	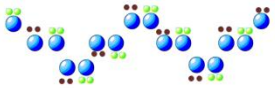	18.5◦ 19.2◦ 20.04◦	(0 2 0) (0 0 2) (1 1 0)	431,512,776,812, 833,840, 1234

polar α phase is dominant in the PVDF films prepared with NMP solvent which is in good agreement with the FTIR results. Moreover, DMSo membrane is showing only one peak at 26.55 which corresponds to (0 2 1) planes of the α phase (Yang *et al*., 2010). Whereas, DMAc shows both α and β phase polymerization, corresponding to the peaks at 18.51 (0 2 0) and 20.7 (1 1 0). From both the characterization of XRD and FTIR it was found that DMF and DMAc are showing both α and β type polymerization whereas, DMSo and NMP are showing only α type polymerization as shown in Table 4, implies that membrane synthesized by DMF and DMAc will be more hydrophobic in nature as compared to other two solvents as β type polymerization enhances the surface roughness and hydrophobicity.

In the case of β- polymerization of PVDF, fluorine and hydrogen atoms were placed in the opposite direction over the carbon chain, as shown in Table 6. Due to the electronegativity of fluorine atoms β- polymerization shows the maximum dipole movement. The dipole movement for α- polymerization is 1.3 D, whereas for β polymerization it is 2.1 D per monomer unit. The difference in electrostatic interactions between the PVDF chain and the solvents may induce the formation of crystalline phases during the immersion process. The membrane prepared with the DMAc and DMF solvent shows β-type polymerization because of the higher dipole movement of both solvents. The dipole movement of solvents used in this experiment was in order, NMP- 4.1 D> DMSo-3.96 D> DMF – 3.86D

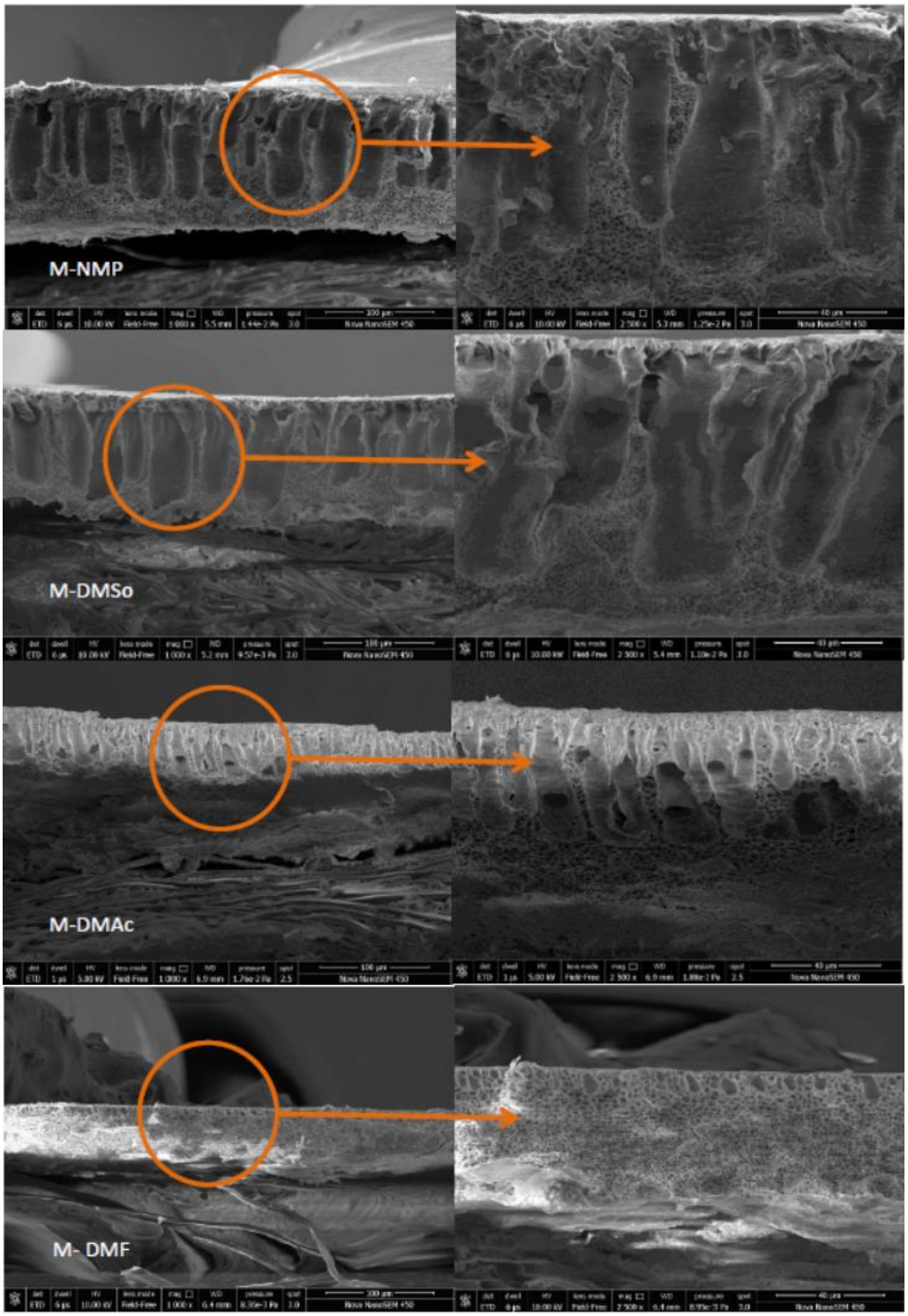

Fig. 5 SEM of the cross-section of the membranes M-NMP, M-DMSo, M-DMAc, and M-DMF at 1000X and 2500X

> DMAc - 3.72D. The crystalline structures of PVDF films were in the order of α, γ, and β phases while increasing the dipole moment of the solvents (Martins *et al*. 2014). Beasause of the reasone NMP and DMSo are showing α- polymerization whereas DMF and DMAc solvent are showing β-type polymerization as shown in Table 5.

From the past analysis, it is evident that DMAc found to be more suitable and competent solvent as compared to other three solvents on the basis of solubility parameter and polymorphism. The cross-section morphology of the PVDF membrane synthesized with different solvents was analyzed using FESEM and is shown in Fig. 5. From the micrographs significant change in the cross-sectional morphologies were observed on using different solvent for membrane synthesis. The SEM micrograph of membrane synthesized by NMP and DMSo is exhibiting long, deep and wide micro-voids beneath the skin layer that grew in length and breadth

Table 6 Table showing polymorphism of membrane prepared with different solvents

Solvent	NMP	DMSo	DMAc	DMF
Polymorphism	α	α	α, β	α, β

Table 7 Properties and parameters of membrane prepared with different solvents

S.no	Membrane code	Solvent	Viscosity (mPa.s)	R_{HSP} (W-S)	Porosity (%)	Contact angle(θ)	Tensile strength (MPa)	Average pore size(μm)
1.	MS-1	NMP	2,43,030	35.64	54.78	89°	102	0.51
2.	MS-2	DMSo	1,35,453	32.62	53.91	85°	103	0.36
3.	MS-3	DMAc	1,07,551	32.51	47.41	92°	106	0.23
4.	MS-4	DMF	1,23,231	31.31	45.63	96°	112	0.14

towards the bottom of the membrane without a well-defined shape. The cross-section of the membrane cast from DMSo was filled with globules of regular shape and size, whereas the cross-section of the membrane cast from NMP was spongy and porous. This structure indicated faster exchange of the solvent and non-solvent at the time of de-mixing. Membrane synthesized with DMAc solvent exhibits a typical asymmetric structure with a combination of plentiful cellular pores in the bulk and micro-voids near the top surface probably owing to liquid-liquid de-mixing. Whereas, M-DMF mainly consists of uniform cellular pores uniform over the entire cross-section part followed by spong-like cavities beneath the cellular pores. And the sponge structure indicates a slow rate of exchange of solvent that remains in the membrane matrix with a non-solvent.

4.1.2 Effect of sdolvent on membrane properties: Tensile strength, Contact angle, Hydrophobicityy

The porosity of membranes prepared with different solvents is shown in Table 7. It is observed that MS-1 (PVDF-NMP) is showing the highest porosity of 54.78%, despite of highest dope viscosity of this combination. This reason can be understood from Table 2 as the Hansen solubility parameter (R_{HSP}) of solvent NMP and water is 35.64. This estimated value is highest among the R_{HSP} of other solvents with water. Therefore, it can be concluded that R_{HSP} kinetic parameter may dominated over the thermodynamic stability of the dope solution. As a result the fast de-mixing will take place during phase inversion process in turns improve the membrane porosity. It was also observed that the viscosity of dope solution for MS-4 (PVDF-DMF) and MS-2 (PVDF-DMSo) are less as compared as compared to MS-1 (PVDF-NMP) as depicted in Table 7. However, the membrane porosity of MS-4 are far less as compared to MS-1 whereas there is no remarkable difference observed in membrane porosity of MS-2 and MS-1. The reason for former case may be understood by the fact that R_{HSP} value is minimum among all solvents which clearly indicate less interaction between solvent and water during coagulation as well as this parameter supersede the kinetic parameter (viscosity). Henceforth, less interconnected globules appeared in the membrane matrix can be further attributed from the Fig. 5. Latter case may be clarified as dope solution viscosity of PVDF-DMSo is far less than PVDF-NMP, therefore, identically the membrane porosity of PVDF-DMSo should be higher, however, the estimated membrane porosity is slightly less as compared to PVDF-NMP. To understand the behaviour of this result, it is necessary to emphasize on de-mixing rate as this phenomena play vital role in finalizing the membrane porosity. On further investigation, it is found that the R_{HSP} value of PVDF-DMSo is 32.62 and PVDF-NMP is 35.64. The difference in R_{HSP} affects more remarkably as compared to the difference in kinetic parameter during phase inversion.

The membrane porosity of PVDF-DMAc is estimated to be 47.41 % which is less as compared to NMP and DMSo. Therefore, it is evident that permeate flux from the PVDF-DMAc is lower as compared to the other two. Further, decrement in the flux may be observed since the estimated average pore size of the PVDF-DMAc membrane is lower as compared to PVDF-NMP and PVDF-DMSo. However, the estimated average pore size is under the desired limit for MD application. It is noteworthy that the contact angle of PVDF-DMAc is 92° which indicates that fabricated membrane is hydrophobic however, other two fabricated membrane contact angle are at the verge of hydrophobicity as a result there may be possibility that pore wetting phenomena may occur at high flow rate. Henceforth, it can be concluded that membrane synthesized from PVDF-DMAc is superior then PVDF-NMP and PVDF-DMSo. Form the Table 7, it can be seen that the membrane characteristics of PVDF-DMAc and PVDF- DMF are approximately identical in terms of membrane porosity and contact angle. However, there is significant difference in average pore diameter of both. It is known that permeate flux varies d_p^2 which will affect the flux to great extent. Hence, suitable trade-off between both the synthesized membranes may be built. On the basis of above fact, it can be attributed clearly that for MD performance, the permeate flux to be higher. Therefore, overall, it can be concluded that DMAc solvent is superior among all the selected solvents for achieving the desired membrane characteristics. It is to mention that in further study the selection of suitable additive was investigated using DMAc as solvent.

4.1.3 Effect of solvent on membrane performance in VMD

To investigate the effect of solvent on the permeability

of PVDF membranes, the pure water flux of the prepared membranes was determined through vacuum membrane distillation and the results are reported in Fig. 6. The pure water fluxes for M0-NMP, M0-DMAc, M0- DMF and M0-DMSO are 26.1, 16.2, 8.8 and 23.3 L/m^{2}h, respectively. Reviewing the research demonstrates that flux through the membranes is mainly affected by many parameters including membrane hydrophobicity, porosity, and the morphology of the membranes. All of these parameters own equal importance and should be considered simultaneously to interpret the permeation behavior of the membranes. As aforementioned, among the membranes, the highest value of the pure water flux is for the membrane prepared using NMP as the solvent (M0-NMP), which can be attributed to the high hydrophobicity and high surface porosity of this membrane, providing a high specific surface area for permeation of water molecules. However, due to its higher pore size, this membrane has a higher risk of wettability. It is important to note that in vacuum membrane distillation (VMD), the driving force for water vapor transfer is the vapor pressure difference across the membrane. In this study, a vacuum was applied on the permeate side, which increased the pressure difference across the membrane, thereby enhancing the driving force for vapor transfer through the membrane. As can be seen in Table 7, M0-DMSo has the highest surface porosity, but due to a higher value of hydrophobicity and surface roughness than M0-NMP causes lower pure water flux for M0-DMSo compared with M0-NMP. According to the results, the M0-DMF shows the lowest pure water flux among the membranes ascribing to its higher hydrophobicity and lower surface porosity compared with other membranes. The characterization results of the membranes demonstrate that the surface roughness, surface porosity, and pore size of the M0-DMAc are in an acceptable range for VMD application, and have a low risk of pore wetting as compared to M0-NMP and M0-DMSO. Despite having high porosity and better flux membrane prepared with both solvents (NMP and DMSO) have a highner risk of pore wetting in VMD application.

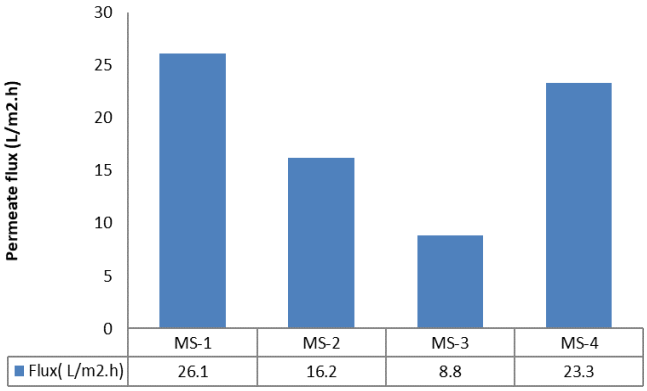

Fig. 6 VMD permeate flux through various membrane prepared using different solvents in dope solution

4.2 Effect of non-solvent additives on membrane Properties

In this work, nine membranes were fabricated using nine different types of additives namely PEG-400, TiO_2, LiCl, LiBr, $AlCl_3$, acetone, ethanol, propanol, and H_2O. These additives were added in PVDF powder and DMAc solvent to make dope solution in order to fabricate flat sheet hydrophobic, micro-porous membrane by NIPS method using sheet casting machine. The fabricated membranes characteristics were identified on the basis of membrane morphology as well as membrane properties such as membrane porosity (ϵ), contact angle (θ), and Tensile strength (TS).

4.2.1 Effect of additive on membrane morphology

The micrographs of all nine fabricated membrane using different additives along with one micrograph without additive are represented in Fig. 7. The nine dope solution were prepared using 16 wt % PVDF powder, 80 wt % DMAc solvent and 4 wt % additive whereas one dope solution is formed with 16 wt % PVDF and 84 wt % DMAc without using any additive. The detail outcomes of the micrographs are shown in Table 8.

The Table 8, illustrated that PEG-400, TiO_2, $AlCl_3$, and H_2O additives may create pore penetration phenomena since broader pore size are formed in the finger like structure of the membrane matrix which may affect the purity of the permeate during desalination using MD. It is also noticed from the micrograph and Table 8 that small globular structure are formed throughout by using TiO_2, and Ethanol whereas big uniformly distributed globular structure in the second layer of the membrane matrix are observed in the micrograph in the case of Propanol as an additive. Therefore, these additives are not supportive enough for better flux since the globular structure hinders the interconnectivity of the pores. Form the micrographs, it is evident that additives namely LiCl, LiBr, and acetone has similar type of morphology. The structure formed by these three additives is asymmetrical which poses top thin layer, deep finger like structure with average pore size followed by sponge like structure underneath. Therefore, the membranes synthesized by using these three additives are recommendable for MD application. However, to investigate the suitable membrane among these three additives, it is necessary to estimate the other required characteristics of the membrane. In the subsequent section, membrane porosity, contact angle and tensile strength were considered for comparison in order to select the best suitable additive for membrane fabrication.

4.2.2 Effect of additive on membrane properties

The developed membrane properties such as membrane porosity, surface contact angle, tensile strength, and average pore size were estimated to identify the best suitable additive for desalination application using MD as shown in Table 9. In the previous section, it was concluded from morphological study that LiCl, LiBr, and acetone are the competent additive among the nine additives. From the comparative Table 9, it is observed that membrane porosity made from LiCl, LiBr, and acetone additives are 48.14%, 47.80%, and 48.8% respectively. Being approximate same membrane porosity values, the contact angle of acetone is highest among three which is 102°. This clearly indicates

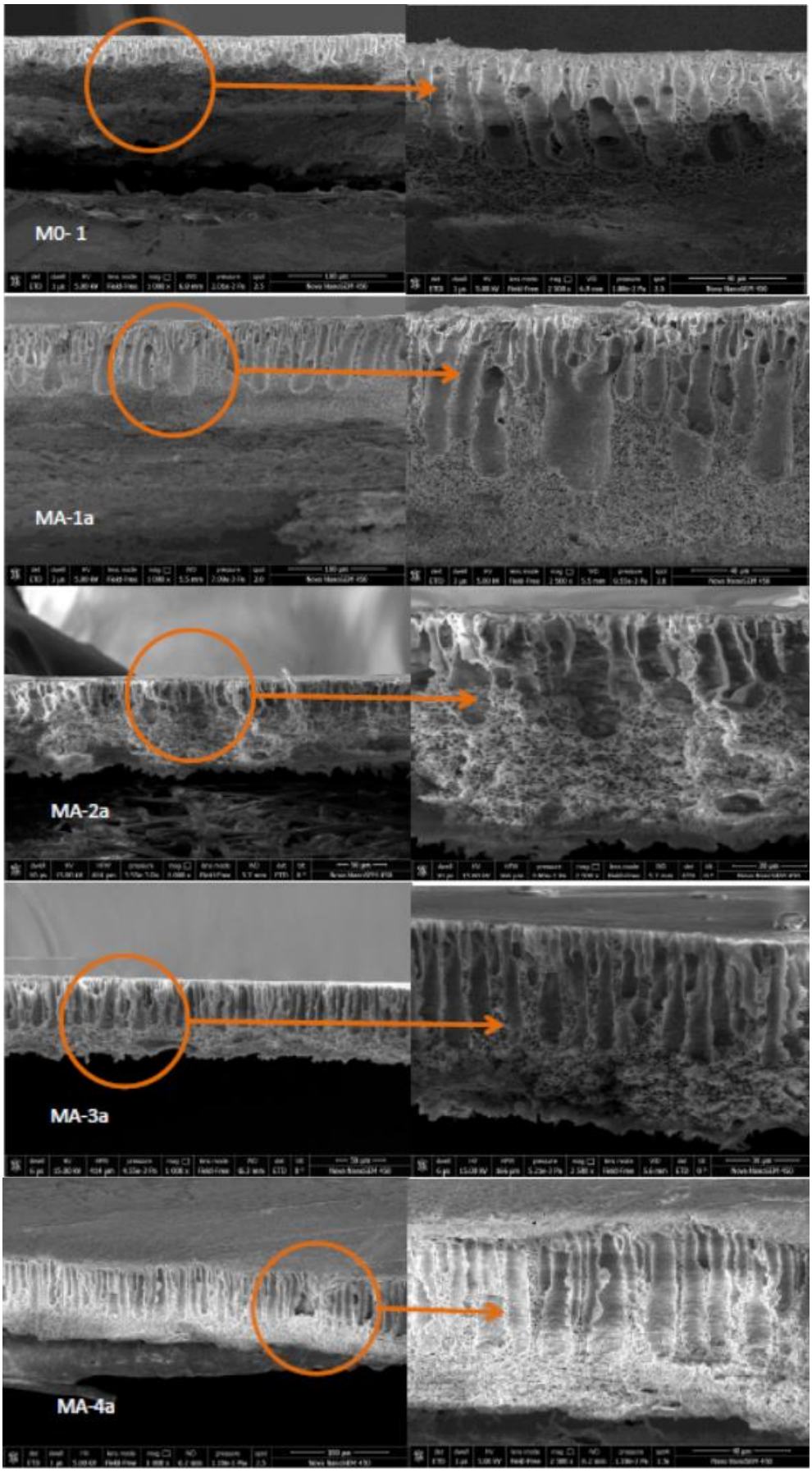

Fig. 7 Membrane morphology using different additives

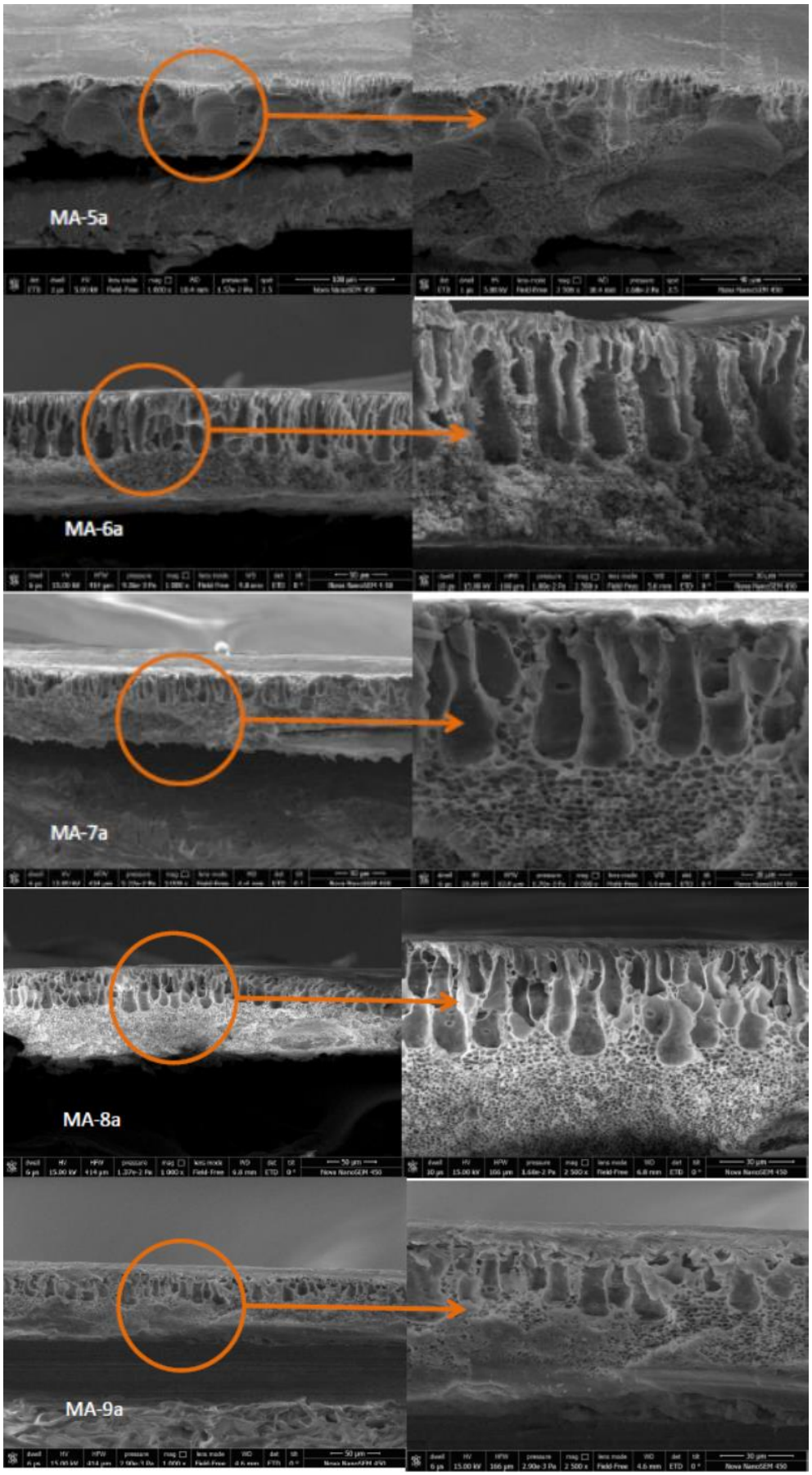

Fig. 7 Continued

Table 8 Study of membrane morphology synthesised by different additive

S.No.	Name of Additives	Top Thin Layer	Middle Finger like structure	Bottom Sponge Structure	Globular Structure
1	PEG-400	Yes	Deeper length and broader pore size	Yes	No
2	TiO_2	No	Deeper length and broader pore size	Yes	Throughout matrix
3	LiCl	Yes	Very deep length and average pore size	Yes (small)	No
4	LiBr	Yes	Very deep length and average pore size	Yes (small)	No
5	$AlCl_3$	Yes	Deepen throughout and very broad pore size	No	No
6	Acetone	Yes	Deeper length and average pore size	Yes	No
7	Ethanol	Yes	Small length and average pore size	Yes	Throughout matrix
8	Propanol	Yes	Average pore size without finger like structure	Yes	Big size Uniformly distributed in second layer
9	Water	Yes	Deeper length and broader pore size	Yes	No
10	Without Additive	Yes	Deeper length and average pore size	Yes	No

Table 9 Estimated membrane properties of synthesized membranes

Membrane code	Additive	Viscosity of dope solution (Cp)	Porosity (%)	Contact angle (°)	Tensile strength (MPa)	Average pore size (µm)	R_{max} (µm)
MA-1	PEG-400	1,55,404	52.67	96	97.3	0.3227	0.51
MA-2	TiO_2	2,44,369	40.14	91	93.3	0.2313	0.42
MA-3	LiCl	2,93,923	48.78	90	98.3	0.213	0.33
MA-4	LiBr	3,76,515	47.80	93	96.3	0.3212	0.57
MA-5	$AlCl_3$	2,43,134	55.23	92	86.4	0.438	1.43
MA-6	Acetone	1,50,891	48.82	102	92.3	0.1844	0.25
MA-7	Ethanol	1,66,886	49.78	87	98.1	0.1367	0.35
MA-8	Propanol	1,31,124	46.42	89	87.5	0.1586	0.37
MA-9	H_20	1,76,453	53.23	104	95.8	0.321	0.67
M0-1	-	1,39,369	42.59	91	98.4	0.2213	0.45

that in comparison of other two additives, the hydro phobicity of membrane restricts the pore wetting phenomena at the top surface. On the other hand the membrane porosity of 48.8 % will additionally create favorable condition for continuous permeate flux. It is also noted form the study that average pore size of the membrane made from acetone is 0.18 micron which is less than membrane fabricated from LiCl and LiBr. This may results in bit lesser permeate flux in the former additive. However, the maximum pore size of LiBr is 0.57 which definitely cause the leakage through the membrane matrix in turns alter the permeate purity during desalination. Due to the hydrophilic nature of LiCl, the membrane contact angle is found to be 90 ° and hence it will be helpful to penetrate the non-volatile solute across the membrane which is not the favorable situation for desalination using MD. Moreover, it is worthful to mentioned that contact angle of membrane fabricated using water as an additive is the highest of value 104°, which is utmost and essential requirement for MD membrane however, the maximum pore size of this membrane is 0.67 micron which despite of high contact angle may create the penetration and pore wetting phenomena along the large pore of the matrix and affects the permeate purity. In contrast to all, acetone has been identified as a volatile additive due to which it allows to form the thin polymeric layer on the top surface which can be illustrated in Fig. 7. This will enhance the resistance to mass transfer of both solvent and non-solvent during phase inversion as a result the narrow pore size at the top surface are forming under the desired range. Therefore, overall it can be conclude that acetone with DMAc solvent is superior among the all selected combination as the membrane characteristics are favorable for MD application.

4.2.3 Effect of additive on membrane performance in VMD

The effect of non- solvent additive on membrane flux through VMD is shown in Fig. 8. All membranes were tested on VMD with a feed concentration of 20 g/l NaCl aqueous solution at feed temperature 80 °C and permeate side vacuum pressure 80 KPa. The flux through the membrane depends on the membrane properties like

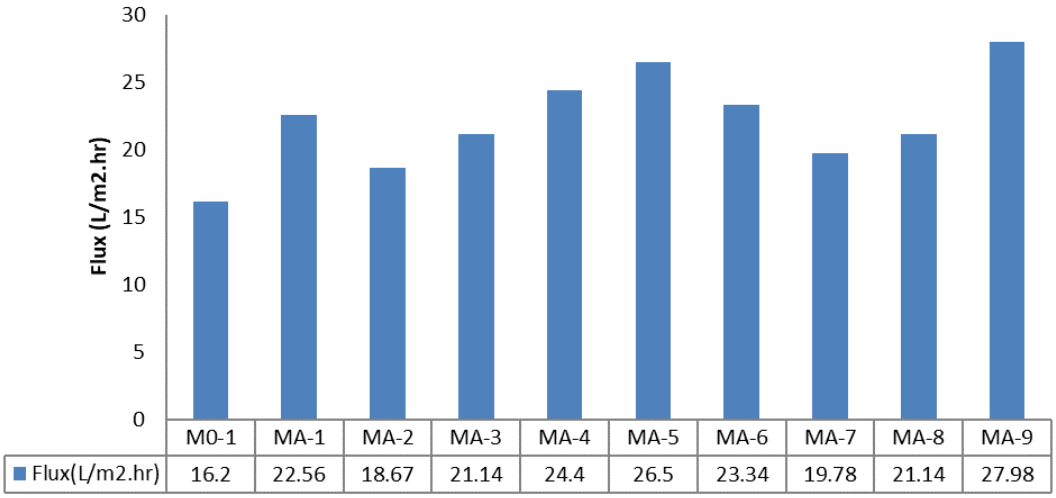

Fig. 8 VMD flux through the different membranes prepared with different additives in dope solution

membrane porosity, hydrophobicity pore size, and morphology. From the Figure. it was observed that permeate flux through the membrane –MA-9 and MA-5 show the highest flux among them, because of their high porosity and pore size, besides flux, they have greater chances of membrane wettability because of their pore structure and hydrophobicity. However, the membrane prepared with acetone as an additive shows better flux and good hydrophobicity with small pore size with fewer chances of membrane wetting. However, a membrane prepared with alcohol as an additive increases the flux to some extent,i.e. MA-7 and MA-8 have to permeate flux of 19.78 and 21.14 L/m^2.hr. Whereas, flux through MA- 3 and MA-4 is 21.14 and 14.4 L/m^2.hr showing that salt additives increase the membrane performance. The rejections to salt were higher than 99.9% for all membranes (M1 to M9).

5. Conclusions

In this study, PVDF hydrophobic microporous membranes with different additives and solvents were synthesized via the NIPS method. The effect of four different solvents namely, DMAc, DMF, DMSO, and NMP on membrane morphology and its characteristics were studied. Along with solvent the effect of different kinds of additives i.e., pore-forming additive (PEG- 400, TiO_2), monovalent and trivalent salt (LiCl, LiBr, $AlCl_3$), low boiling point additive, was investigated in terms of membrane morphology, properties, and VMD testing. The following conclusions were reached during this work:

• The polymorphism and crystalline phase of synthesized PVDF membranes could be well regulated by different solvents. NMP favors the formation of α phases, DMAc and DMF solvent shows β-type polymerization because of the higher dipole movement of both solvents whereas DMSo favors β phase confirmed by FTIR and XRD analysis.

• The morphology and membrane structure of the synthesized membrane depends on the exchange rate of solvent and non-solvent at the time of demixing. The membrane cast from DMSo shows long thin finger-like pores whereas the membrane prepared with NMP shows a smaller globular structure.

• Pore-forming additives, like PEG-400 and TiO_2, increase the porosity along with the pore size of the membrane.

• Inorganic salt addition in the dope solution increases the porosity with long finger-like pores. Pore size of the synthesized membrane depends upon the size of the additive, trivalent salt creates a larger pore size compared to monovalent salts.

• Acetone came out to be a better additive because of its volatile nature it forms a thin layer of polymeric film at the top surface which increases the hydrophobicity of the membrane surface. This thin film also provides resistance to mass transfer of solvent and non-solvent at the time of phase inversion.

• Organic weak non-solvent additives like ethanol and propanol react with the polymer chain due to the presence of a hydroxylic group and induce pre-gelation so that the resulting membrane has higher porosity with inter-connectivity.

• The pre-gelation impact is more significant when strong non-solvent H20 was used as an additive. The synthesized membrane has high porosity and good interconnectivity resulting in high permeate flux but due to bigger pore size have a high risk of membrane wettability.

• The permeate flux through the different membranes with various additives varies from 16.2 to 27.98 kg/m^2.hr., but membranes with higher pore sizes have a risk of membrane wettability. So, the membrane prepared with acetone as an additive shows a better permeate flux of 23.34 kg/m^2.hr with better porosity, hydrophobicity, and fine pore structure.

Acknowledgments

The authors are also extremely grateful to the Material research center (MRC) at MNIT for for all the facilities to determine SEM micrographs, Tensile strength determination.

References

Baghel, R., Kalla, S., Upadhyaya, S., Chaurasia, S.P. and Singh, J. (2017), "Treatment of Sudan III dye from wastewater using vacuum membrane distillation", *J. Basic Appl. Eng. Res.*, **4**(3), 237-241.

Chunsheng, F.,Wang, R., Shi, B., Li, G. and Wu, Y. (2006), "Factors affecting pore structure and performance of poly (vinylidene fluoride-co-hexafluoro propylene) asymmetric porous membrane", *J. Membr. Sci.*, **277**(1-2), 55-64. https://doi.org/10.1016/j.memsci.2005.10.009.

Diyana, K., Hashim, N., Ong, B., Kakihana, Y., Higa, M. and Matsuyama, H. (2021), "Multiple effect of thermal treatment approach on PVDF membranes: Permeability enhancement and silver nanoparticles immobilization", *J. Environ. Chem. Eng.*, **9**(4), 105769. https://doi.org/10.1016/j.jece.2021.105769.

Fernández, G., García-Payo, L. and Khayet, M. (2014), "Effects of mixed solvents on the structural morphology and membrane distillation performance of PVDF-HFP hollow fiber membranes", *J. Membr. Sci.*, **468**, 324-338. https://doi.org/10.1016/j.memsci.2014.06.014.

Hazlina, J., Nik, J., Abdul, A., Ismail, A., Othman,M., Rahman, M., Aziz, F., Yusof, N. and Daud, N. (2021), "Porous polyether sulfone for direct methanol fuel cell applications: Structural analysis", *Int. J. Energy Res.*, **45**(2), 2277-2291. https://doi.org/10.1002/er.5921.

Kalla, S. (2020), "Use of membrane distillation for oily wastewater treatment - A review", *Biochem. Pharm.*, 104641. https://doi.org/10.1016/j.jece.2020.104641.

Kuiling, L., Hou, D., Fu, C., Wang, K. and Wang, J.(2019), "Fabrication of PVDF nanofibrous hydrophobic composite membranes reinforced with fabric substrates via electrospinning for membrane distillation desalination", *J. Environ. Sci.*, **75**, 277-288. https://doi.org/10.1016/j.jes.2018.04.002.

Lei Du, H., Li, Y., Guo, M., Zhou, J. and Qiao, S. (2023), "Superhydrophobic PVDF membrane formed by crystallization process for direct contact membrane distillation", *IScience*, **26**(5), 106464. https://doi.org/10.1016/j.isci.2023.106464.

Loussif, N. and Orfi, J. (2016), "Comparative study of air gap, direct contact and sweeping gas membrane distillation configurations", *Membr. Water Treat.*, **7**(1), 71-86. https://doi.org/10.12989/mwt.2016.7.1.071.

Marek, G. (2011), "Water desalination by membrane distillation", *Desalination*, 302017. https://doi.org/10.5772/14746.

Phattaranawik, J., Jiraratananon, R. and Fane, A.G. (2003), "Heat transport and membrane distillation coefficients in direct contact membrane distillation", *J. Membr. Sci.*, **212**(1-2), 177-193. https://doi.org/10.1016/S0376-7388(02)00498-2.

Rasool, M. and Vankelecom, F.J. (2021), "Preparation of full-bio-based nanofiltration membranes", *J. Membr. Sci.*, **618**, 118674. https://doi.org/10.1016/j.memsci.2020.118674.

Sadrzadeh, M. and Bhattacharjee,S. (2013), "Rational design of phase inversion membranes by tailoring thermodynamics and kinetics of casting solution using polymer additives", *J. Membr. Sci.*, **441**, 31-44. https://doi.org/10.1016/j.memsci.2013.04.009.

Sajjad, M., Safekordi, A., Tavakolmoghadam, M., Rekabdar, F. and Hemmati, M. (2016), "Comparison of the membrane morphology based on the phase diagram using PVP as an organic additive and TiO2 as an inorganic additive", *Polymer*, **97**, 559-568. https://doi.org/10.1016/j.polymer.2016.05.069.

Shu Yuan, P., Haddad, A., Kumar, A. and Wang, S. (2020), "Brackish water desalination using reverse osmosis and capacitive deionization at the water-energy nexus", *Water Res.*, **183**, 116064. https://doi.org/10.1016/j.watres.2020.116064.

Tae, J., Kim, J.,Wang, H., Nicolo, E., Drioli, E. and Lee, Y. (2016), "Understanding the non-solvent induced phase separation (NIPS) effect during the fabrication of microporous PVDF membranes via thermally induced phase separation (TIPS)", *J. Membr. Sci.*, **514**, 250-263. https://doi.org/10.1016/j.memsci.2016.04.069.

Tibi, F., Charfi, A., Cho, J. and Kim, J. (2020), "Fabrication of polymeric membranes for membrane distillation process and application for wastewater treatment : Critical review", *Proc. Safe Environ. Protect.*, **141**, 190-201. https://doi.org/10.1016/j.psep.2020.05.026.

Tofighy, M., Mohammadi, T. and Sadeghi, M.H. (2021), "High-flux PVDF/PVP nanocomposite ultrafiltration membrane incorporated with graphene oxide nanoribbones with improved antifouling properties", *J. Appl. Polym. Sci.*, **138**(4), 1-15. https://doi.org/10.1002/app.49718.

Wang, J., Zheng, L., Wu, Z., Zhang, Y. and Zhang, X. (2016), "Fabrication of hydrophobic flat sheet and hollow fiber membranes from PVDF and PVDF-CTFE for membrane distillation", *J. Membr. Sci.*, **497**, 183-193. https://doi.org/10.1016/j.memsci.2015.09.024.

Wang, X., Chen, D., He, T., Zhou, Y., Tian, L., Wang, Z. and Cui, Z. (2023), "Preparation of lateral flow PVDF membrane via combined vapor- and non-solvent-induced phase separation (V-NIPS)", *Membranes*, **13**(1). https://doi.org/10.3390/membranes13010091.

Yadav, M. and Upadhyay, S. (2023), "Process optimization for fabrication of PVDF-TiO_2 hydrophobic membrane using phase inversion method for desalination application using VMD", *Mater. Today Proc.*, **90**, 39-50. https://doi.org/10.1016/j.matpr.2023.06.153

Yadav, M., Upadhyay, S., Singh, K., Chaturvedi, T.K. and Vashishtha, M. (2022), "Morphological study of synthesized PVDF membrane using different non-solvents for coagulation", *Membr. Water Treat.*, **13**(4), 173. https://doi.org/10.12989/mwt.2022.13.4.173

Yadav, M., Upadhyaya, S. and Singh, K. (2024), "Enhancing the hydrophobicity and surface roughness of synthesized PVDF membrane using evaporation and non-solvent-induced phase separation", *Arab. J. Sci. Eng.*, **49**(6), 8189-8200. https://doi.org/10.1007/s13369-024-08726-y.

Yong Soo, K., Kim, K. and Kim, U.(1991), "Asymmetric membrane formation via immersion precipitation method. I. kinetic effect", *J. Membr. Sci.*, **60**(2-3), 219-232.

Zhenghui, L., Xiang, J., Hu, X., Cheng, P., Zhang, L., Du, W., Wang, S. and Tang, N. (2021), "Effects of coagulation-bath conditions on polyphenylsulfone ultrafiltration membranes", *Chinese J. Chem. Eng.*, **34**, 332-340. https://doi.org/10.1016/j.cjche.2020.11.038.

Zoungrana, A., Zengin, I., Elcik, H., Yesilirmak, D., Karadag, D. and Çakmakci, M. (2016), "Arsenic removal from drinking water by direct contact membrane distillation", *Membr. Water Treat.*, **7**(3), 241-255. https://doi.org/10.12989/mwt.2016.7.3.241.

CC